

## Anisotropic Ionic Conductivity in Block Copolymer Membranes by Magnetic Field Alignment

Pawel W. Majewski, Manesh Gopinadhan, Woo-Sik Jang, Jodie L. Lutkenhaus,<sup>‡</sup> and Chinedum O. Osuji\*

*Department of Chemical and Environmental Engineering, Yale University, New Haven, Connecticut 06511, United States*

Received August 13, 2010; E-mail: chinedum.osuji@yale.edu

**Abstract:** The self-assembly of diblock copolymers provides a convenient route to the formation of mechanically robust films with precise and tunable periodic arrangements of two physically demixed but chemically linked polymeric materials. Chemoselective transport membranes may be realized from such films by selective partitioning of an active species into one of the polymer domains. Here, lithium ions were selectively sequestered within the poly(ethylene oxide) block of a liquid crystalline diblock copolymer to form polymer electrolyte membranes. Optimization of the membrane conductivity mandates alignment of self-assembled structures such that conduction occurs via direct as opposed to tortuous transport between exterior surfaces. We show here that magnetic fields can be used in a very simple and scalable manner to produce highly aligned hexagonally packed cylindrical microdomains in such membranes over macroscopic areas. We systematically explore the dependence of the ionic conductivity of the membrane on both temperature and magnetic field strength. A surprising order of magnitude increase in conductivity relative to the nonaligned case is found in films aligned at the highest magnetic field strengths, 6 T. The conductivity of field aligned samples shows a nonmonotonic dependence on temperature, with a marked decrease on heating in the proximity of the order–disorder transition of the system before increasing again at elevated temperatures. The data suggest that domain-confined transport in hexagonally packed cylindrical systems differs markedly in anisotropy by comparison with lamellar systems.

### Introduction

The development of solid polymer electrolytes for rechargeable battery applications is driven by key issues of safety and mechanical stability of current state of the art liquid electrolytes.<sup>1,2</sup> The generally lower mobility of ions in solids versus liquids however is a significant drawback in the utilization of solid electrolytes. One solution to this problem involves the use of nanoencapsulation, whereby self-assembly of a block copolymer (BCP) provides a locally liquid medium for the transport of ionic species within a material that is mechanically robust on macroscopic scales. While early work in this area relied on the use of relatively soft secondary blocks,<sup>3–5</sup> it was subsequently shown that mechanical and electrical properties could be decoupled, permitting the use of stiff, glassy blocks to provide mechanical integrity.<sup>6</sup> The characteristic morphology of the material (interfacial curvature and spacing) is controlled by the composition and molecular weight of the block copolymer chain.

The most commonly exploited ion conductive BCPs display lamellar (LAM) or hexagonally packed cylindrical (HEX) morphologies. For lithium ion conduction, the ion-transporting domain is often formed by doping poly(ethylene oxide) (PEO) using lithium salts. Such chemoselective transport has long been envisioned as a potential use of block copolymers. Optimization of the conductivity of the polymer electrolyte membrane involves alignment of the self-assembled morphology such that conduction occurs via direct as opposed to tortuous transport between the exterior surfaces of the system as depicted in Figure 1a.

There are only a few reports concerning measurements of anisotropic conductivity in aligned self-assembled soft materials. Anisotropy ratios as high as 450 were observed between perpendicular and parallel conductivities of cylindrical PEO microdomains in films of micrometer-scale thickness which spontaneously align due to surface forces.<sup>7</sup> This ratio decreased with increasing Li-doping as lithium ions were increasingly solubilized in the non-PEO domains. Spontaneous surface driven homeotropic anchoring of a polymerizable mesogen bearing an oligo-oxyethylene spacer was used to produce an aligned liquid crystalline (LC) polymer film in which lithium ions were

<sup>‡</sup> Current Address: Artie McFerrin Department of Chemical Engineering, Texas A&M University, College Station, TX 77843.

- (1) Croce, F.; Appetecchi, G. B.; Persi, L.; Scrosati, B. *Nature* **1998**, *394* (6692), 456–458.
- (2) Zhang, S. S. *J. Power Sources* **2007**, *164* (1), 351–364.
- (3) Soo, P. P.; Huang, B. Y.; Jang, Y. I.; Chiang, Y. M.; Sadoway, D. R.; Mayes, A. M. *J. Electrochem. Soc.* **1999**, *146* (1), 32–37.
- (4) Ruzette, A. V. G.; Soo, P. P.; Sadoway, D. R.; Mayes, A. M. *J. Electrochem. Soc.* **2001**, *148* (6), A537–A543.
- (5) Trapa, P. E.; Huang, B. Y.; Won, Y. Y.; Sadoway, D. R.; Mayes, A. M. *Electrochem. Solid State Lett.* **2002**, *5* (5), A85–A88.
- (6) Singh, M.; Odusanya, O.; Wilmes, G. M.; Eitouni, H. B.; Gomez, E. D.; Patel, A. J.; Chen, V. L.; Park, M. J.; Fragouli, P.; Iatrou, H.;

Hadjichristidis, N.; Cookson, D.; Balsara, N. P. *Macromolecules* **2007**, *40* (13), 4585.

(7) Li, J.; Kamata, K.; Komura, M.; Yamada, T.; Yoshida, H.; Iyoda, T. *Macromolecules* **2007**, *40* (23), 8125–8128.

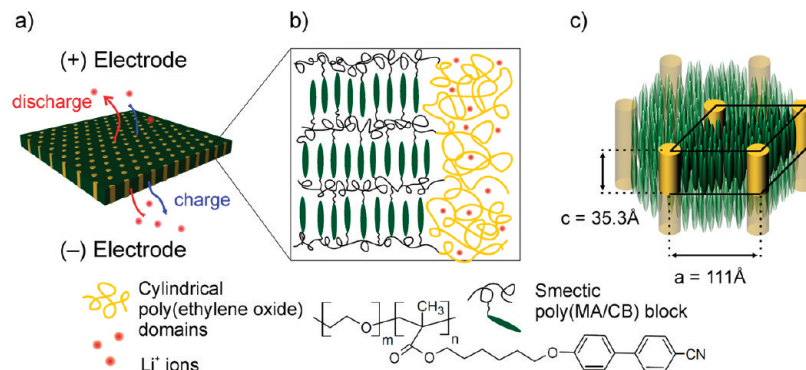


**Figure 1.** (a) Structure of the PEO-*b*-PMA/CB block copolymer membrane with lithium-conducting poly(ethylene oxide) cylindrical domains aligned uniformly in the current flow direction. (b) The zoomed-in views show the details of the structure of the polymer. (c) The liquid-crystalline unit cell with mesogenic backbone residues anchored in the layers transverse to the long axes of PEO cylinders.

complexed with the oxyethylene domain.<sup>8</sup> This system yielded conductivity anisotropy ratios up to 4500 at elevated temperatures. Measurements in direct methanol fuel cell membranes constructed from spontaneously aligned sulfonated styrene triblock copolymers showed a factor of 10 difference in the in-plane versus out-of-plane proton conductivities.<sup>9</sup> More recently, Balsara et al. have examined anisotropic proton transport in a lamellar forming coil-coil diblock copolymer aligned by electric fields, shearing, and mechanical pressing.<sup>10</sup> A maximum anisotropy ratio of  $\sigma_{\perp}$  to  $\sigma_{\parallel}$  of 75 was found for hot pressed films. Crucially, this work also considered the ratio between the high conductivity aligned state and the isotropic or random state produced by simple solution casting of the polymer. The measured enhancement over the isotropic conductivity was found to be only 40% in the best case but consistent with a simple geometric argument regarding an effective medium representation of lamellar systems.<sup>11,12</sup> Other workers have reported an enhancement of the isotropic proton conductivity by a factor of 10 in a study of an electric-field poled polymer blend system.<sup>13</sup> The effects of spontaneous parallel orientation in lamellar films of sulfonated styrene-isoprene-styrene triblock copolymers on proton conductivity have also been considered.<sup>14</sup>

The scarcity of data regarding anisotropic conductivity in structured soft materials along with the exciting potential for these materials in energy applications provides strong motivation for work in this area. In this context, the inability to reliably control orientational ordering in block copolymers over the relevant length scales (>1 mm) and with the geometrical specificity required remains a significant challenge to be overcome.<sup>15</sup> This is a long-standing problem in soft materials, and it is particularly acute in scenarios where out-of-plane or vertical alignment of 1D nanostructures is required in thin film geometries, as desirable for ionic conduction in polymer membranes. This is a challenging regime where typical methods

such as mechanical shear alignment cannot be applied and electric field alignment is hindered by issues of scalability and dielectric breakdown. In contrast to electric fields, the absence of dielectric breakdown concerns with magnetic fields permits a more flexible exploitation of the general space pervasive nature of electromagnetic fields. The resulting absence of electrode contact issues thus enables the application of an externally imposed magnetic driving force without the geometric constraints encountered with either electric fields or mechanical shear. Magnetic fields are thus particularly attractive for the realization of vertically aligned structures in thin film geometries. They offer great flexibility in their application,<sup>16,17</sup> and their utilization can be easily scaled to the continuous processing of large area films. Here, we use magnetic fields to produce vertically aligned Li<sup>+</sup> conducting cylindrical domains in a block copolymer film over millimeter length scales. This results in materials with highly oriented morphologies that display an order of magnitude improvement in conductivity relative to randomly oriented samples. We characterize the field and temperature dependence of the anisotropic conductivity. The results are consistent with the phase behavior of the block copolymer overall and help to define a parameter space for magnetic field-based processing of ion transport polymers of this type.

## Experimental Section

**Materials.** Poly(ethylene oxide-*b*-6-(4'-cyanobiphenyl-4-yloxy)-hexyl methacrylate) PEO-*b*-PMA/CB 10.4 kg/mol, PDI = 1.15,  $f_{\text{PEO}} = 0.23$  was supplied by Polymer Source. The as-received material was dissolved in 50 mL of dichloromethane and extracted with three 50 mL portions of deionized water to remove postsynthetic inorganic salt impurities. The solvent was evaporated under mild vacuum at room temperature followed by vacuum drying ( $10^{-2}$  mbar) at 90 °C for 48 h. The final vacuum-drying step was performed at 110 °C for 24 h, and the sample-containing desiccator was transferred into an argon-purged glovebox (<1 ppm O<sub>2</sub>, <1 ppm H<sub>2</sub>O). Lithium perchlorate (LiClO<sub>4</sub>) (battery grade, 99.99%) and dimethyl formamide (DMF) (anhydrous, 99.8%) were used as-received from Sigma-Aldrich.

**Preparation of LiClO<sub>4</sub> Doped Polymer Samples.** The sample preparation was conducted inside the glovebox, including the assembly of hermetic cells for SAXS, conductivity, and DSC studies. A controlled amount of 0.5% solution of LiClO<sub>4</sub> was mixed

- (8) Kishimoto, K.; Yoshio, M.; Mukai, T.; Yoshizawa, M.; Ohno, H.; Kato, T. *J. Am. Chem. Soc.* **2003**, *125* (11), 3196–3197.  
 (9) Elabd, Y. A.; Walker, C. W.; Beyer, F. L. *J. Membr. Sci.* **2004**, *231* (1–2), 181–188.  
 (10) Park, M. J.; Balsara, N. P. *Macromolecules* **2010**, *43* (1), 292–298.  
 (11) Sax, J.; Ottino, J. M. *Polym. Eng. Sci.* **1983**, *23* (3), 165–176.  
 (12) Wanakule, N. S.; Panday, A.; Mullin, S. A.; Gann, E.; Hexemer, A.; Balsara, N. P. *Macromolecules* **2009**, *42* (15), 5642–5651.  
 (13) Umeda, M.; Uchida, I. *Langmuir* **2006**, *22* (10), 4476–4479.  
 (14) Elabd, Y. A.; Napadensky, E.; Walker, C. W.; Winey, K. I. *Macromolecules* **2005**, *39* (1), 407.  
 (15) Darling, S. B. *Prog. Polym. Sci.* **2007**, *32*, 1152–1204.

- (16) Gopinadhan, M.; Majewski, P. W.; Osuji, C. O. *Macromolecules* **2010**, *43* (7), 3286–3293.  
 (17) Majewski, P. W.; Osuji, C. O. *Langmuir* **2010**, *26* (11), 8737–8742.

with polymer DMF solutions and cast onto glass Petri dishes. The solvent was evaporated using the vacuum desiccator for 24 h initially at 60 °C and then at 90 °C for another 48 h.

**Assembly of Conductivity and SAXS Cells.** Each cell consisted of two highly polished aluminum plates separated by a 400  $\mu\text{m}$  thick double-sided sticky PTFE spacer with a circular ( $\phi = 6.5$  mm) opening, cell constant  $k = 0.120 \text{ cm}^{-1}$ . A controlled amount of the polymer was molded into the cell at elevated temperature, covered with the second electrode, and the entire assembly was gently pressed together.

**Magnetic Alignment.** The magnetic alignment experiments were performed with a superconducting electromagnet capable of reaching 6 T static field (American Magnetics Inc.). The SAXS and conductivity cells were mounted on a thermostated aluminum block allowing control of orientation of the cells with respect to the field, i.e. parallel or perpendicular. In all runs the samples were subject to the same temperature profile starting with a brief ramp to 85 °C followed by slow cooling to room temperature at 0.1 °C/min rate. The “randomly” aligned samples were thermally annealed in the same manner in the absence of the magnetic field.

**Small Angle X-ray Scattering.** Small angle X-ray scattering (SAXS) experiments were carried out using a Rigaku S-3000 system with a pinhole-collimated (0.7 mm) Cu  $K\alpha$  source and 2-D electronic wire detector permitting, in our configuration, access to a range of scattering vectors from 0.02 to 0.4  $\text{\AA}^{-1}$ . Radial integration of the scattered intensity was rendered using MATLAB routines (Rigaku) with silver behenate as a 58.38  $\text{\AA}$   $d$ -spacing standard.

**Differential Scanning Calorimetry and Polarized Optical Microscopy.** The thermal behavior of the system was studied using DSC Q200 (TA Instruments) at a heating rate of 20 °C/min. Aligned samples were examined in transmission mode with crossed polarizers under 20 $\times$  magnification with a Zeiss Axio Observer microscope equipped with a CCD camera. The samples were confined between two glass slides with a spacer between them to prevent shear induced alignment. Pixel values from recorded micrographs were averaged to provide the transmission intensity. Following established practice,<sup>18</sup> transmission intensities were normalized by the empty beam intensity  $I_0$ . This was measured with the polarizer and analyzer in the parallel configuration, with no sample present.

**Atomic Force Microscopy (AFM).** AFM was performed using a Multimode AFM with a Nanoscope IIIa controller (Veeco) under tapping mode (phase imaging) in air with standard Si probes (TESPA, Veeco). Samples were prepared by freeze fracture in liquid nitrogen.

**Conductivity Measurements.** The cells with the aligned polymer were mounted on a thermostated two electrode stage connected to a Solartron 1260 analyzer operating in a 0.1–10<sup>6</sup> Hz frequency range at the amplitude of 100 mV. The conductivity of the films was calculated using a value of electrical resistance obtained by fitting the data to the equivalent circuit model with the ZPlot software. Conductivity temperature scans were performed in 3 °C increments at a 0.5 °C/min heating rate with an equilibration time of 3 min at each measurement point.

## Results and Discussion

Our system is a poly(ethylene oxide-*b*-methyl acrylate) block copolymer in which the methyl acrylate segments are derivatized by a cyanobiphenyl mesogen, PEO-*b*-PMA/CB. The mesogen forms a thermotropic smectic A mesophase within the MA/CB domain, which is the origin of the anisotropy in diamagnetic susceptibility that permits alignment by the magnetic field.<sup>16</sup> The ethylene oxide segments in the PEO block form complexes with lithium cations blended into the system, rendering the material ion conductive. The polymer displays a hexagonally

packed cylindrical morphology, consisting of PEO domains embedded in the LC matrix. As inferred from the small-angle X-ray scattering (SAXS) data the cyanobiphenyl mesogens exhibit homogeneous (planar) anchoring at the intermaterial dividing surface (IMDS) and so the smectic layers are arranged with their director parallel to the long axis of the cylinders as shown schematically in Figure 1b. PEO crystallinity was significantly suppressed in the unadulterated material and was not observable with differential scanning calorimetry (DSC), polarized optical microscopy (POM), or wide-angle X-ray scattering as studied here. Significant undercooling of the material below room temperature or extended quiescent periods (>3 weeks) at ambient conditions did result in some crystallization of the PEO chains as evidenced by the emergence of weak melting peaks in DSC. Complexation with lithium typically results in further suppression of any kinetically limited PEO crystallinity,<sup>19–21</sup> and so in these experiments overall the semicrystalline nature of PEO did not play a discernible role. This is consistent with the presence of a well resolved glass transition temperature around –56 °C (SI Figure 2). The neat diblock shows an endothermic peak at 68 °C on heating due to the smectic–isotropic LC transition. Temperature dependent SAXS reveals that this LC transition is concurrent with the order–disorder transition (ODT) via which the block copolymer structure is thermally destabilized. The coincidence of LC clearing temperature and block copolymer ODT is attributed to the low molar mass of the polymer. It has similarly been observed in measurements on a lamellar forming system of the same chemistry<sup>16</sup> and in other LC BCPs as well.<sup>22–24</sup> Previous studies of PEO containing block copolymers report stabilization of microphase separated structures due to an increased Flory  $\chi$  parameter resulting from sequestration of lithium on formation of the  $\text{Li}^+$ –ether oxygen complex.<sup>25</sup> No such effect however was observed for the PEO-*b*-PMA/CB materials over the range of stoichiometries considered here, and the ODT was independent of sample composition up to 24:1 EO:Li<sup>+</sup>. However at higher salt content, EO:Li<sup>+</sup> 16:1, an increase of the clearing temperature to 72 °C was observed.

In the alignment experiments, the polymer was heated beyond  $T_{\text{ODT}}$  and then slowly cooled to room temperature in the presence of the field. 2D SAXS data for the 120:1 EO:Li<sup>+</sup> material is shown in Figure 2 as a function of field strength. Examination of the peak intensity and fwhm show that a field strength in excess of 3 T is required to generate noticeable alignment of the system. At the highest fields of 4, 5, and 6 T, sharp reflections in the small angle regime along the meridional line originate from highly oriented PEO cylinders aligned with their long axes parallel to the field while the scattering along the equatorial direction is due to the aligned smectic layers with their director or layer-normal aligned also along the applied field direction. The improvement in the order of the system due to

(18) Garetz, B. A.; Newstein, M. C.; Dai, H. J.; Jonnalagadda, S. V.; Balsara, N. P. *Macromolecules* **1993**, *26* (12), 3155.

(19) Chen, J.; Frisbie, C. D.; Bates, F. S. *J. Phys. Chem. C* **2009**, *113* (10), 3903–3908.

(20) Guilherme, L. A.; Borges, R. S.; Moraes, E. M. S.; Silva, G. G.; Pimenta, M. A.; Marletta, A.; Silva, R. A. *Electrochim. Acta* **2007**, *53* (4), 1503–1511.

(21) Kumar, B.; Rodrigues, S. J.; Koka, S. *Electrochim. Acta* **2002**, *47* (25), 4125–4131.

(22) Zheng, W. Y.; Hammond, P. T. *Macromolecules* **1998**, *31* (3), 711–721.

(23) Anthamatten, M.; Hammond, P. T. *Macromolecules* **1999**, *32* (24), 8066–8076.

(24) Hamley, I. W.; Castelletto, V.; Lu, Z. B.; Imrie, C. T.; Itoh, T.; Al-Hussein, M. *Macromolecules* **2004**, *37* (13), 4798–4807.

(25) Young, W. S.; Epps, T. H. *Macromolecules* **2009**, *42* (7), 2672–2678.

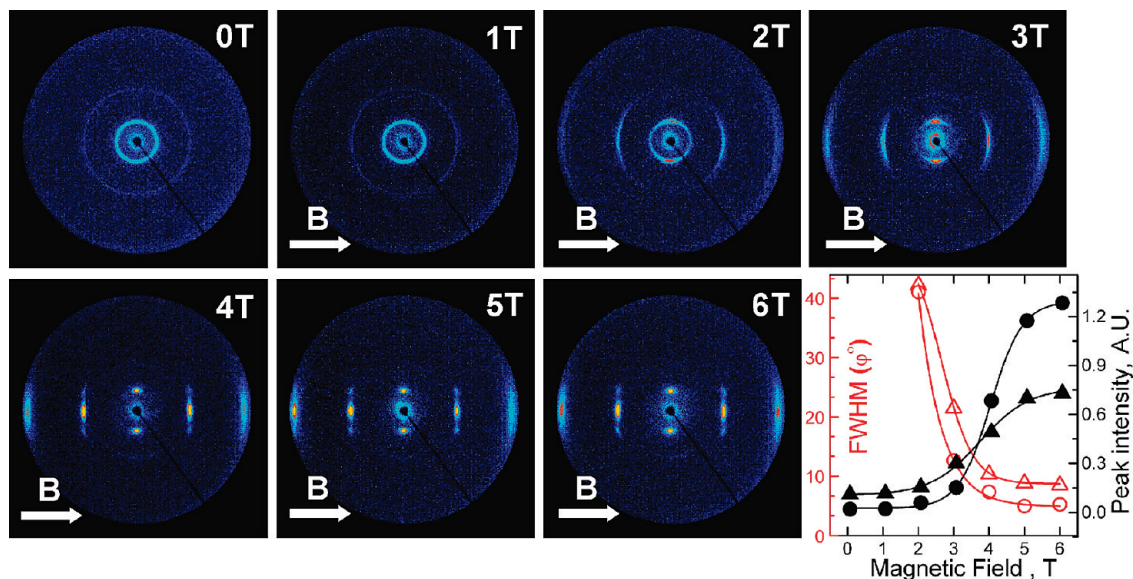


**Figure 2.** Evolution of two-dimensional SAXS patterns as a function of the applied magnetic field strength during alignment of PEO(120 EO:Li<sup>+</sup>)-b-PMA/CB. The field direction, indicated by the arrows, is horizontal with respect to the orientation of the X-ray detector. The inset shows the variation of the peak intensities of the microdomain scattering at  $q = 0.07 \text{ \AA}^{-1}$  (triangles) and LC scattering (circles) at  $q = 0.18 \text{ \AA}^{-1}$  as a function of field strength. The open symbols represent the fwhm parameter extracted from a Lorentzian fit of the data. Lines are provided from spline fits as guides to the eye.

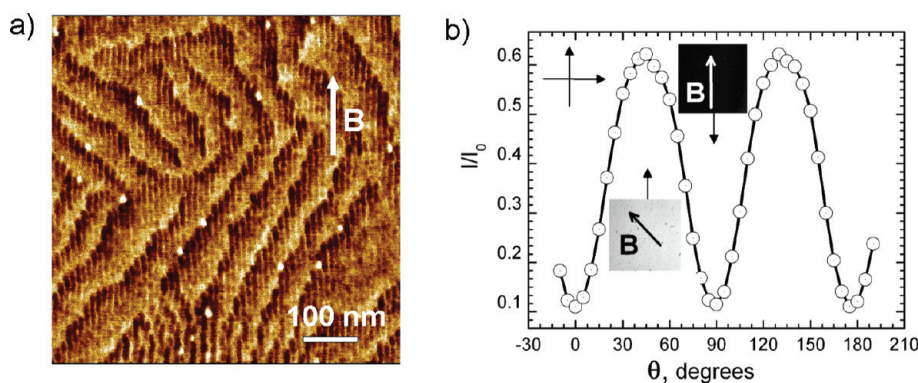


**Figure 3.** (a) Phase contrast AFM of the cross-sectional view of neat PEO-*b*-PMA/CB material aligned in a 5 T field. The thin bright stripes correspond to PEO cylindrical domains. The field was applied vertically in the image plane as indicated. (b) The transmitted intensity of the aligned PEO-*b*-PMA/CB sample under crossed polarized light against the angle ( $\theta$ ) between the magnetic field direction and the polarizer shows periodic variation at every 90° indicating strong alignment of the mesogens along the field direction over large areas. Micrographs span roughly a 1.5 mm field of view. The sample rotation axis is parallel to the optical axis of the microscope.

the influence of the field is rather pronounced. Such is the enhancement that the diagonal reflections are clearly resolved at  $q = 0.19 \text{ \AA}^{-1}$ . These reflections are due to contributions from the orthogonal variations of the microdomain and smectic layer electron densities and appear in the 2D data as small apparent satellites to the smectic scattering along the equatorial line. The SAXS pattern is consistent with a planar (homogeneous) anchoring of the biphenyl mesogens at the block interface (IMDS), depicted in Figure 1c, and their positive diamagnetic susceptibility anisotropy ( $\Delta\chi > 0$ ). The smectic LC ordering in the system under the uniaxial magnetic field imposes a macroscopic unidirectional orientation of EO cylindrical microdomains. Integration of the 2D SAXS patterns taken with the beam incident along the magnetic field direction (SI Figure 1b) shows reflections with ratios of reciprocal spacing  $1:\sqrt{3}:\sqrt{4}:\sqrt{7}$  indicating hexagonally packed cylindrical PEO microdomains with a  $d$ -spacing of  $d = 96 \text{ \AA}$  from which the cylinder-to-cylinder spacing can be calculated using  $d_0 = (4/3)^{1/2}d$ . Assuming equal densities of the semicrystalline PEO

and liquid crystalline PMA/CB, the estimated volume fraction of the PEO domains is  $\phi = 0.23$ . This is related to the cylinder radius,  $r$ , by  $\phi = (2\pi/\sqrt{3})(r/d_0)^2$ . For the neat PEO-*b*-PMA/CB,  $d_0 = 111 \text{ \AA}$  and  $r = 28 \text{ \AA}$ . Cross-sectional AFM imaging revealed cylindrical PEO microdomains oriented along the applied field direction, Figure 3a. The average cylinder spacing is estimated to be  $110 \text{ \AA}$ , in good agreement with SAXS measurements. The  $d$ -spacing of the system decreased slightly with the doping level (from  $96 \text{ \AA}$  for neat diblock to  $89 \text{ \AA}$  for 16:1 EO:Li<sup>+</sup>). By contrast, the spacing between the smectic layers,  $35.3 \text{ \AA}$ , was independent of LiClO<sub>4</sub> doping.

POM confirms that the strong alignment deduced by SAXS is uniform on macroscopic scales, over the full 6.5 mm extent of the sample. The birefringence of the neat aligned sample displays strong anisotropy under crossed polarizers, Figure 3b. The periodic modulations in light transmission with sample orientation are observed due to corresponding periodic variation in the smectic layer orientation relative to the plane polarization of the incident light. A smooth sinusoidal variation between

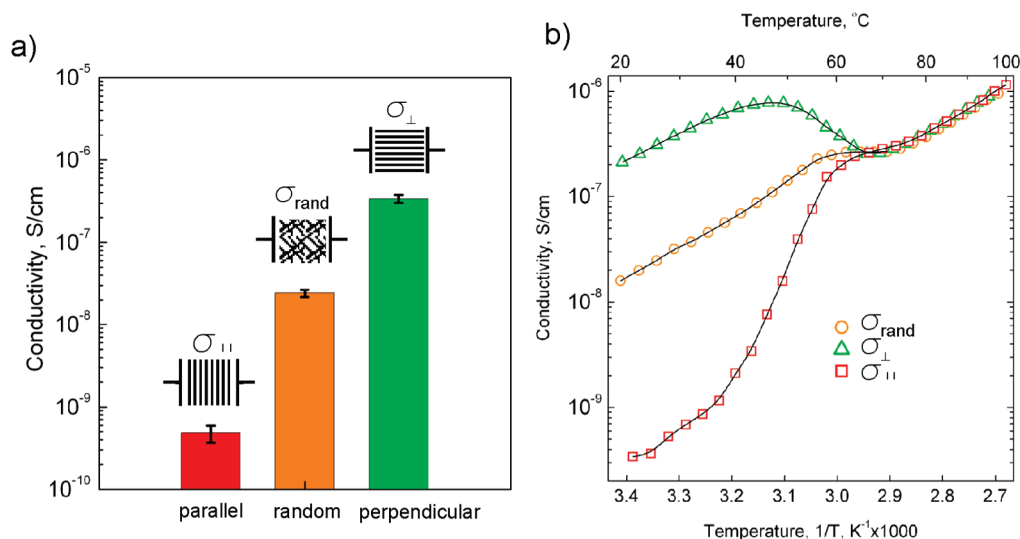


**Figure 4.** (a) The average room temperature electrical conductivity of 120:1 EO:Li<sup>+</sup> sample aligned in 5 T magnetic field in two orthogonal directions; nonaligned material's conductivity shown for comparison. Error bars represent standard deviation of  $\sigma$  for at least three independent alignment experiments. (b) Temperature dependence of conductivities shown in Arrhenius convention ( $x$ -axis reversed). Lines are added as a visual guide.

the minima and maxima separated by 45° and the large absolute amplitude of the variation are good indications that the system is well aligned over the large areas observed.

Initial expectations for anisotropic conductivity were based on an effective medium argument which predicts a 2-fold increase in conductivity of aligned cylindrical domains over isotropic ones and a 50% enhancement in lamellar systems.<sup>11</sup> Indeed, recent data for proton conductivity are suggestive of an apparent limit of 50% for the improvement of conductivity in aligned lamellar materials.<sup>10</sup> Contrary to initial expectations however, the aligned cylindrical PEO-*b*-PMA/CB system here displays roughly a 10-fold increase in conductivity relative to the unaligned samples, Figure 4. At room temperature, the conductivity of the polymer with parallel PEO cylinders (long axis of the cylindrical microdomains transverse to the current flow) is a further order of magnitude smaller than that of the unaligned material. We carefully verified the reproducibility of both the alignment procedure and the conductivity measurements. Good consistency was achieved in both, as highlighted by standard deviations not exceeding  $\pm 10\%$  for  $\sigma_{\perp}$  and  $\sigma_{\text{rand}}$ . For parallel alignment the magnitude of the error ( $\pm 20\%$ ) originates primarily from the uncertainty of the fit value of the  $\sigma_{\parallel}$  due to the much higher electrical resistance of the samples. The highly anisotropic charge transport results from the near monodomain structure of the polymer produced by field alignment as indicated by SAXS data (Figure 2) and is consistent with confinement of the ionic transport to the interior of the PEO domains. By contrast, any intercylinder conduction is limited by the high resistance of the weakly polar surrounding matrix.

The temperature dependent conductivity of the two aligned samples and randomly oriented material is presented for the 120:1 EO:Li<sup>+</sup> sample in Figure 4b. The overlap above the clearing temperature is expected as the samples undergo a phase transition to the disordered melt. The merging of these three curves for  $T > T_{\text{ODT}}$  was consistently reproducible and underlines the reliability of the experimental setup for performing temperature resolved measurements. Moreover, the temperature dependent conductivity of aligned samples on cooling from above  $T_{\text{ODT}}$  follows the same trajectory traced by that of the

random, nonaligned samples on initial heating (SI Figure 3). This highlights the fact that the samples are indeed well isotropized by heating above  $T_{\text{ODT}}$ . Although there is a slightly higher slope discernible at low temperatures ( $T < 40$  °C) for the parallel aligned case, it can be said that, within experimental error, all three traces possess the same slope. This indicates that the mechanism of conduction is the same in all three cases and suggests that the minimal conductivity in the parallel aligned material originates from percolation of PEO domains via remnant defects.  $\sigma_{\perp}$  and  $\sigma_{\parallel}$  display an intriguing behavior in the 15–20 °C temperature window immediately preceding  $T_{\text{ODT}}$ . The perpendicularly aligned sample has initially higher  $\sigma$  than that at  $T_{\text{ODT}}$  for all samples. If one assumes there is no significant change in the activation energy for conduction below and above ODT, as suggested by recent reports for coil–coil diblocks,<sup>12</sup> then by definition the conductivity must go through a maximum en route to rejoining a line of the same initial slope. Likewise, for the parallel alignment which has initially lower  $\sigma$  than that at  $T_{\text{ODT}}$  for all samples, the data should show an increase and an inflection point on increasing temperature before resuming a largely unchanged gradient. This is precisely what is observed in both cases. Strikingly, the peak in  $\sigma_{\perp}$  appears to coincide with the inflection point in  $\sigma_{\parallel}$  and the initial uptick in  $\sigma_{\parallel}$  with the first deviation of  $\sigma_{\perp}$  from its low temperature slope. The randomly oriented sample shows a small 5 °C regime before  $T_{\text{ODT}}$  in which the conductivity is largely insensitive to temperature. These measurements were conducted in a quasi-static manner using long equilibration times (>300 s) at each of the closely spaced temperature points and thus do not appear to reflect kinetic effects. The same characteristic features were observed across a range of stoichiometries for which a detailed report will be presented elsewhere. Intriguingly, the temperature dependent changes in conductivity for perpendicularly aligned samples are completely reversible without hysteresis on cooling for temperatures below  $T_{\text{ODT}}$ , Figure 5. This, along with a lack of discernible change in SAXS data in this regime, rules out any hypothetical irreversible disruption of the alignment due to disordering for  $T < T_{\text{ODT}}$ .

The origin of the temperature dependent behavior in advance of the ODT is unclear. A possible explanation is

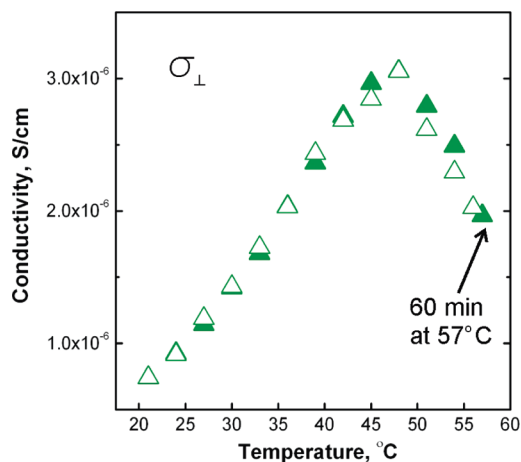


**Figure 5.** Evolution of the conductivity of the perpendicularly aligned 50:1 EO:Li<sup>+</sup> sample heated up to 57 °C ( $T_{\text{ODT}} = 65$  °C) (▲) and cooled down to room temperature (Δ) in the absence of the field. The reversible overlap of both plots indicates the stability of conductive domain orientation and suggests that the drop in  $\sigma_{\perp}$  preceding  $T_{\text{ODT}}$  is not induced by an irreversible thermal disruption of the ordered blocks.

the diffusion of ions outside of PEO cylinders driving a depletion of carriers and resulting in a drop of conductivity of the perpendicularly aligned sample. Such a repartitioning of ions would act to increase the conductivity of the parallelly aligned samples as it would facilitate ion migration through the nonconductive material. We speculate however that these nonmonotonic displays are best interpreted in terms of morphological changes occurring in the samples, and not in terms of any apparent activation energy or solute repartitioning on increasing temperature. Although SAXS does not show large scale changes in the structure of the sample in this temperature regime, it is possible that local changes, particularly conformational changes due to enhanced layer fluctuations in the smectic mesophase, may play a role here. It is notable that although reports to date in coil–coil diblocks do not observe a strong change in apparent transport activation energies on crossing the ODT,<sup>4,12</sup> these studies do not involve aligned systems. Aligned LC systems by contrast do show nonmonotonic behavior in the vicinity of clearing temperatures.<sup>7,8</sup>

Examining the influence of field strength yields the expected result that higher fields lead to better conductivity for perpendicularly aligned samples. Comparison of the plot in Figure 6b with SAXS data (Figure 2) allows one to relate the charge transport properties to the anisotropic morphology. Consistent with the SAXS data, an initial rise in conductivity at 2 T and saturation at approximately 5T are observed. Figure 6a depicts the field dependent conductivity of the neat material at 45 °C. This temperature was chosen as the conductivity of the neat diblock at room temperature was so low that its electrical resistance was beyond the nominal measurable range and the resulting readings were thus not entirely reliable. The small but measurable conductivity of the neat diblock can be explained by the presence of residual impurities that were not removed during the purification of the material, or possible contamination during the cell's assembly. Nevertheless, the neat sample shows an almost 3 orders of magnitude lower conductivity than the 120:1 EO:Li<sup>+</sup> doped material. Most significantly, the field required for saturation of the aligned conductivity increases with increased Li<sup>+</sup> doping, in an approximately linear fashion, above 120:1 EO:Li<sup>+</sup> (SI Figure 4). As a result, with the further increase of lithium salt content one can anticipate the need to utilize increasingly stronger fields, or better optimized alignment processes for maximization of the conductivity.

## Conclusion

The realization of practical solid polymer electrolyte membranes requires the continued development of materials chemistry as well as materials processing to control the nano- or microstructures involved. Our work here has demonstrated the facile production of macroscopic films with a highly aligned nanostructure which leads to a significant improvement over the conductivity performance of unaligned materials. The effect of magnetic field strength on morphology and conductivity has been quantitatively explored. This work contributes to recent efforts to rigorously quantify the impact of morphology and alignment on the bulk electrical transport properties of self-assembled soft materials for electrolytic membrane applications.<sup>10,12,26</sup> The origin of the disparity between predicted and observed anisotropy ratios for these cylinder forming materials is intriguing but currently unclear. The issue warrants further study, and future work will address the question of anisotropic conductivities in aligned lamellar morphologies for

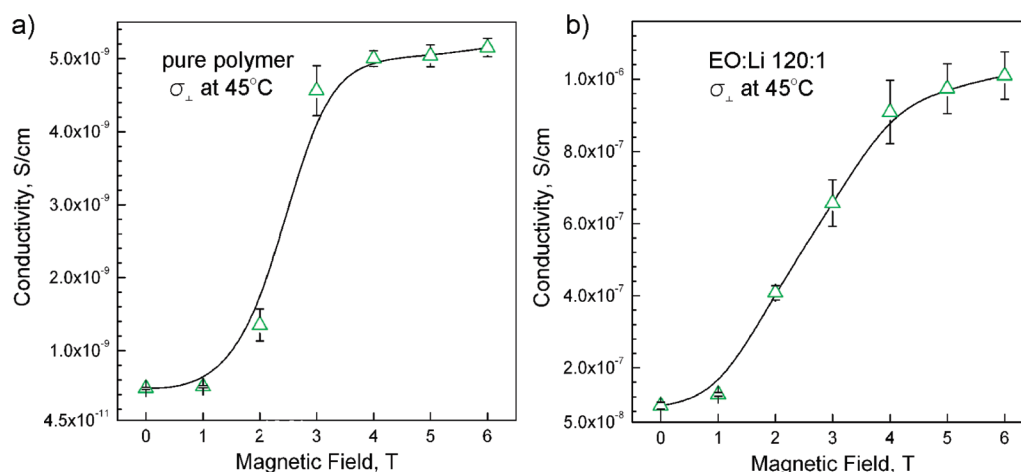


**Figure 6.** Electrical conductivity at 45 °C of the block copolymer with the PEO domains aligned perpendicular to electrodes' surface as a function of magnetic field strength used for alignment. (a) Neat PEO-*b*-PMA/CB, (b) 120:1 EO:Li<sup>+</sup> sample. Error bars in plots symbolize the experimental error calculated for three repetitions of the alignment at a given field strength. Splines are added as eye guides.

comparison. Additionally, the role of LC disorder in the temperature dependent conductivity needs to be further elucidated if these materials are to be of practical relevance in the future. Decoupling the LC clearing temperature from the ODT by increasing the molecular weight of the polymer can provide insight in this regard.

**Acknowledgment.** The authors gratefully acknowledge insightful discussions with Prof. Nitash Balsara of UC Berkeley, Prof.

---

(26) Park, M. J.; Balsara, N. P.; Jackson, A. *Macromolecules* **2009**, *42* (17), 6808–6815.

Thomas Epps of Delaware, and Prof. Venkat Ganesan of UT Austin as well as funding support from NSF via DMR-0847534 (P.M., M.G., and C.O.). Technical support from American Magnetics Inc. is also gratefully acknowledged.

**Supporting Information Available:** Figures showing SAXS data for the neat diblock copolymer and DSC data. This material is available free of charge via the Internet at <http://pubs.acs.org>.

JA107309P